PCCP

Cite this: *Phys. Chem. Chem. Phys.*, 2012, **14**, 15180–15184

www.rsc.org/pccp

PAPER

Connecting the (quantum) dots: towards hybrid photovoltaic devices based on chalcogenide gels†

Jilian N. De Freitas,[a] Lasantha Korala,[b] Luke X. Reynolds,[c] Saif A. Haque,[c] Stephanie L. Brock*[b] and Ana F. Nogueira*[a]

Received 28th August 2012, Accepted 11th September 2012
DOI: 10.1039/c2cp42998e

CdSe(ZnS) core(shell) aerogels were prepared from the assembly of quantum dots into mesoporous colloidal networks. The sol–gel method produces inorganic particle interfaces with low resistance to electrical transport while maintaining quantum-confinement. The photoelectrochemical properties of aerogels and their composites with poly(3-hexylthiophene) are reported for the first time.

Organic solar cells based on conjugated polymers are among the most promising devices for solar energy conversion. The "classical" device consists of a bulk-heterojunction of a polymer–fullerene network, comprising poly(3-hexylthiophene) (P3HT) and the soluble fullerene derivative [6,6]-phenyl C_{61}-butyric acid methyl ester ($PC_{61}BM$). The introduction of small alkyl thiol molecules, optimization of solvent conditions, and use of conjugated copolymers with smaller band gaps along with $PC_{71}BM$ enabled significant improvements in the efficiency of these devices, reaching ~7%.[1,2] However, bottlenecks such as morphology control, the mismatch with the solar spectrum and stability still persist.

The easily tunable optical properties, high extinction coefficients, electron affinity and intrinsic dipole moments of inorganic semiconductor quantum dots (QDs), as well as their potential for multiple exciton generation make QDs such as CdSe,[3,4] $CuInSe_2$,[5] PbS,[6] and PbSe[7] promising alternatives to organic fullerene derivatives in hybrid solar cell devices. The addition of QDs in polymer solar cells should enhance the light-harvesting, thus offering the possibility of higher photocurrents. However, the highest efficiencies achieved for this kind of QD-based solar cells are still around 3%,[8–11] mainly due to the poor charge transport properties of the inorganic phase, where transport occurs by hopping through a percolation pathway. Realization of a highly-interconnected pathway is a great challenge because the surface ligands used to passivate the QD surfaces have highly insulating, long aliphatic chains. Improved device performance *via* surface modification has been achieved by exchange with smaller ligands (*e.g.* alkyl amines,[12] pyridine,[3,4] benzenedithiol[10]), shortening of long chain groups by thermal cleavage,[13] or removal of excess surface groups by performing additional washing steps.[14] The performance improves due to the reduction of inter-particle distances which then enhances the charge transport. The synthesis of QDs directly in the polymer solution[15] or the deposition of films from polymer solutions that also contain a soluble precursor to the inorganic nanoparticles[16–18] have also been conducted to achieve QD dispersions with polymers and without passivating ligands. In lieu of being an electroactive component, QDs may also be used as a third component in polymer–fullerene devices, where they act only as sensitizers.[19]

Brock and co-workers have employed sol–gel methods to assemble chalcogenide QDs into gels, xerogels and aerogels where QDs form a percolation network with inorganic particle interfaces that do not present the barriers to electrical transport (endemic in organic-ligated QDs), yet remain quantum-confined.[20,21] In this work, the properties of mixtures of CdSe(ZnS) core(shell) aerogels and P3HT are investigated for the first time using photoelectrochemistry and transient absorption spectroscopy, and their suitability to photovoltaic applications is discussed.

CdSe(ZnS) core(shell) QDs were synthesized according to literature methods with slight modifications[22,23] and then treated with a basic 11-mercaptoundecanoic acid (MUA) solution to achieve ligand exchange with the thiolate. After removing excess ligands, QDs were dispersed in methanol and gelation was initiated by adding tetranitromethane (TNM). Wet gels were aged for several days, exchanged with acetone to remove by-products, followed by liquid CO_2 exchange and drying by supercritical extraction, resulting in the formation of aerogels. Detailed experimental procedures are given in the ESI.†

[a] *Chemistry Institute, University of Campinas, Campinas, P.O Box 6154, 13083970, Brazil. E-mail: anaflavia@iqm.unicamp.br*
[b] *Department of Chemistry, Wayne State University, Detroit, MI 48202, USA. E-mail: sbrock@chem.wayne.edu*
[c] *Centre for Plastic Electronics and Department of Chemistry, Imperial College London, SW72AZ, London, UK*

† Electronic supplementary information (ESI) available: Experimental procedures, FTIR spectrum and TEM images of CdSe(ZnS) aerogel, absorption spectra of P3HT:QDs films, chronoamperometry of QD, aerogel, P3HT and P3HT:CdSe (core only aerogel) films, scheme of charge transfer processes and morphological analysis. See DOI: 10.1039/c2cp42998e

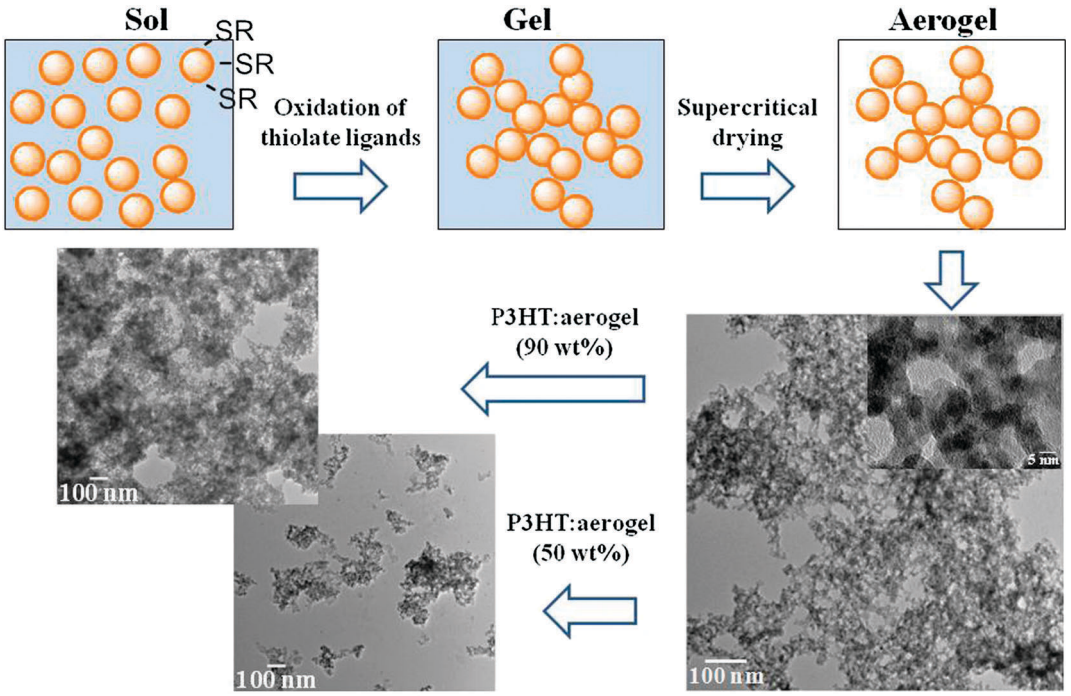

Fig. 1 Schematic representation of the synthesis of aerogels from MUA-capped QDs and HRTEM images of (right) CdSe(ZnS) aerogels and (left) P3HT:aerogel mixtures containing 50 wt% or 90 wt% of CdSe(ZnS). The scale bar indicates 5 nm (inset) or 100 nm (all other images).

Fig. 1 schematically represents the sol–gel transformation of QDs, initiated by oxidation of surface thiolate ligands by TNM. Removal of surface groups is followed by the solvation of surface Zn^{2+} ions. Further oxidation of S^{2-} on the QD surfaces links the QDs together *via* disulfide/polysulfide species, forming the gel network. The formation of chalcogenide linkages at the interfaces during gelation has been verified with XPS and Raman studies.[24] Supercritical drying of wet gels results in aerogels. The process of gelation and supercritical drying removes the majority, but not all, of the capping groups, as is evident from FTIR spectroscopy (Fig. S1, ESI†). Generally, about ~15% (by mole) of the ligands remain.[25] The residual ligands are present on the surface of the gel network, not at the interface, and are not expected to impact particle–particle conductivity, although they may have a significant effect on charge separation at the interface between the gel and P3HT.

High-resolution transmission electron microscopy (TEM) was employed to image the aerogels and their mixtures with P3HT (Fig. 1 and Fig. S2, ESI†). The presence of end to end connected QDs (joints) is visible in the TEM images. End to end connections lead to a more penetrating network for the aerogels, compared to QDs, especially in samples with lower concentrations of inorganic materials. Importantly, mixing with P3HT does not disrupt the gel network.

The absorption spectra of CdSe(ZnS) QDs and aerogels (dispersed in toluene) and P3HT (film) are shown in the inset in Fig. 2. The absorption profile of the aerogels is similar to that of the QDs used to prepare the gels. The first excitonic peak at ~615 nm indicates that each nanocrystal in the aerogel network is ~5.3 nm in diameter;[26,27] *i.e.*, the quantum confinement effects of the respective nanometer scale building blocks are almost fully maintained despite aggregation into a 3-D connected network, as previously observed.[28] The inorganic

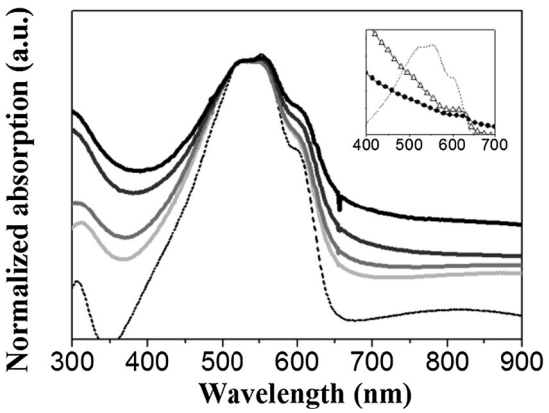

Fig. 2 Steady-state absorption spectra of hybrid films of P3HT:aerogel with different weight ratios of CdSe(ZnS): (···) 0 wt%, (—) 50 wt%, (—) 67 wt%, (—) 80 wt% and (—) 90 wt%. Spectra are normalized by the fraction of photons absorbed at 550 nm. The inset shows the absorption of a pristine P3HT film and toluene solutions of (Δ) QDs or (●) aerogel.

materials harvest light in the wavelength region coincident with the $\pi \rightarrow \pi^*$ transition of P3HT (maximum at 550 nm) and the shoulder attributed to vibronic species (maximum at 600 nm). Fig. 2 shows the steady-state absorption spectra as a function of increasing CdSe(ZnS) concentration in P3HT:aerogel hybrid films. There is an enhancement in light scattering as the CdSe(ZnS) : P3HT ratio is increased. P3HT:QDs hybrid films show a similar behaviour (Fig. S3, ESI†). In solar cells, light scattering can increase the optical path length within the active layer, offering the possibility of enhanced absorption and, thus, enhanced photocurrent generation.

To investigate the photoelectrochemical properties, chronoamperometry measurements were obtained in a three-electrode cell connected to a potentiostat. Ag/AgCl and a Pt wire were employed as a reference and counter electrode, respectively, and a 0.1 M aqueous solution of Na_2SO_4 saturated with O_2 was used as electrolyte. Working electrodes with an active area of 1 cm^2 were prepared by either drop-casting or spin-casting dispersions onto ITO (indium tin oxide) coated glass. The current characteristics were recorded as a function of time, while repeated on–off cycles of light illumination were applied. First, aerogels, QDs and P3HT were analysed individually. The original organic ligand-capped QD films showed negligible photocurrent response upon light illumination, indicative of poor charge transport properties within the films. In order to remove excess ligands, extra washing steps were employed, leading to some aggregation of the QDs and an improved photocurrent response. Aerogel and QD films show n-type behaviour, while P3HT presents p-type behaviour, consistent with a preferential charge transport of electrons in the inorganic materials and holes in the polymer film (Fig. S4, ESI†).

Fig. 3 shows chronoamperometry measurements of P3HT:CdSe(ZnS) hybrid films containing different concentrations of aerogels or QDs by weight. Similar experiments were performed

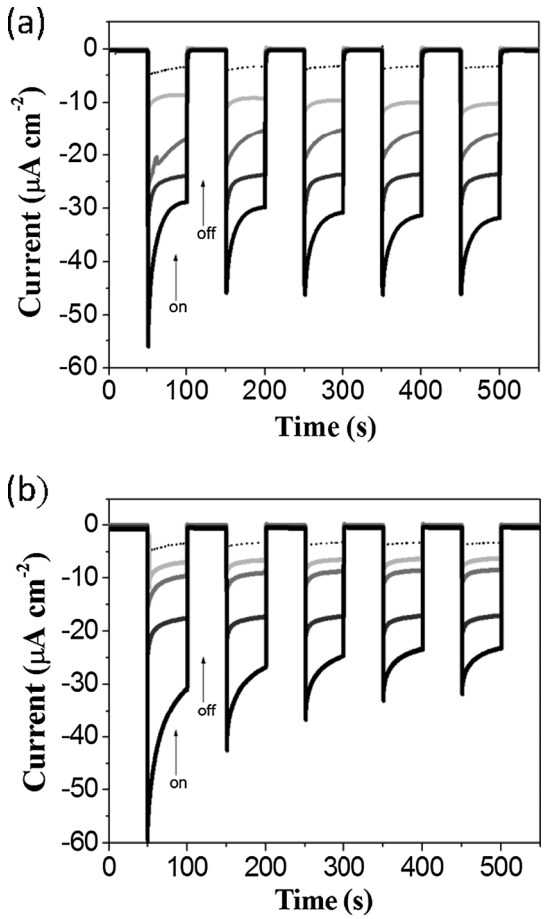

Fig. 3 Photocurrent responses under white light (100 mW cm^{-2}) of films of (a) P3HT:aerogel or (b) P3HT:QDs, with (···) 0 wt%, (—) 50 wt%, (—) 67 wt%, (—) 80 wt% and (—) 90 wt% of CdSe(ZnS), in the presence of a 0.1 M Na_2SO_4 electrolyte saturated with O_2.

for mixtures of P3HT:CdSe (core only) aerogels, however lower photocurrents were observed (Fig. S5, ESI†). This may be due to the reduction of non-radiative recombination achieved by passivating the surface states, since the shell layer reduces the presence of traps on the QD (and aerogel) surfaces[28] and also facilitates the injection of electrons from P3HT.[29]

Bare P3HT electrodes produce significantly lower currents than photoelectrodes assembled with hybrid films. The dramatically increased p-type photocurrent in the hybrid system stems from effective charge carrier separation *via* charge transfer between P3HT and the inorganic materials, which increases the formation of polarons in the polymer phase. It has been shown that the incorporation of CdSe QDs in P3HT films increases the hole current and switches the transport from field dependent mobility to an energy trap model.[30] A scheme of the expected charge transfer processes in these systems is provided in Fig. S6 (ESI†).

Interestingly, the systems containing P3HT:aerogel and P3HT:QD behave differently as the concentration of the inorganic material increases. At low concentrations of inorganic materials ($\leq$80 wt%), the photocurrents delivered by P3HT:aerogel electrodes are higher than those delivered by P3HT:QD electrodes. This is related to the formation of a percolation network, required for efficient charge transport. For aerogel-based samples, some percolation paths are preformed during the synthesis of the gel, while for QD-based samples, the percolation limit is typically achieved only at very high concentrations of QDs (*e.g.*, the best photovoltaic responses are usually obtained when $\sim$90 wt% of QDs are incorporated into the polymer matrix[4,17,31]). When the concentration reaches 90 wt%, the photocurrent of the QD-based electrode becomes similar to the aerogel-based electrode. Under this condition, both samples achieved effective formation of 3-D interconnected networks. It is worth noting that there is some degree of QD aggregation in the P3HT:QD electrodes, due to partial removal of surface ligands.

Microsecond to millisecond laser-based transient absorption spectroscopy (TAS) was used to determine the yield of charge pair generation and the charge recombination dynamics following photoexcitation of the P3HT–metal chalcogenide films. TAS kinetic traces were taken using a simultaneous pump and probe setup (details given in ESI†). Optical excitation at 510 nm resulted in the formation of a broad transient absorption band centred at $\sim$950 nm (Fig. 4c) which can be assigned to the P3HT polaron.[32–34] We note that a contribution from the excitation of the inorganic phase, followed by injection of holes into the polymer,[35] cannot be ruled out. The charge recombination dynamics were obtained by monitoring the decay of the 980 nm band. The data shown in Fig. 4a and b follow the charge recombination reaction between the photogenerated holes in the P3HT and the electrons in the CdSe(ZnS), as a function of increasing aerogel or QDs concentration. The amplitude of the signal (magnitude of change in optical density, ΔOD) in Fig. 4 can be directly related to the number of photogenerated charge pairs formed. It is clear that in both cases the yields of photogenerated charge improve upon increasing the CdSe(ZnS) weight fraction. Generally, at lower concentrations of inorganic material, higher yields of charge generation are observed using aerogels. It is also apparent that

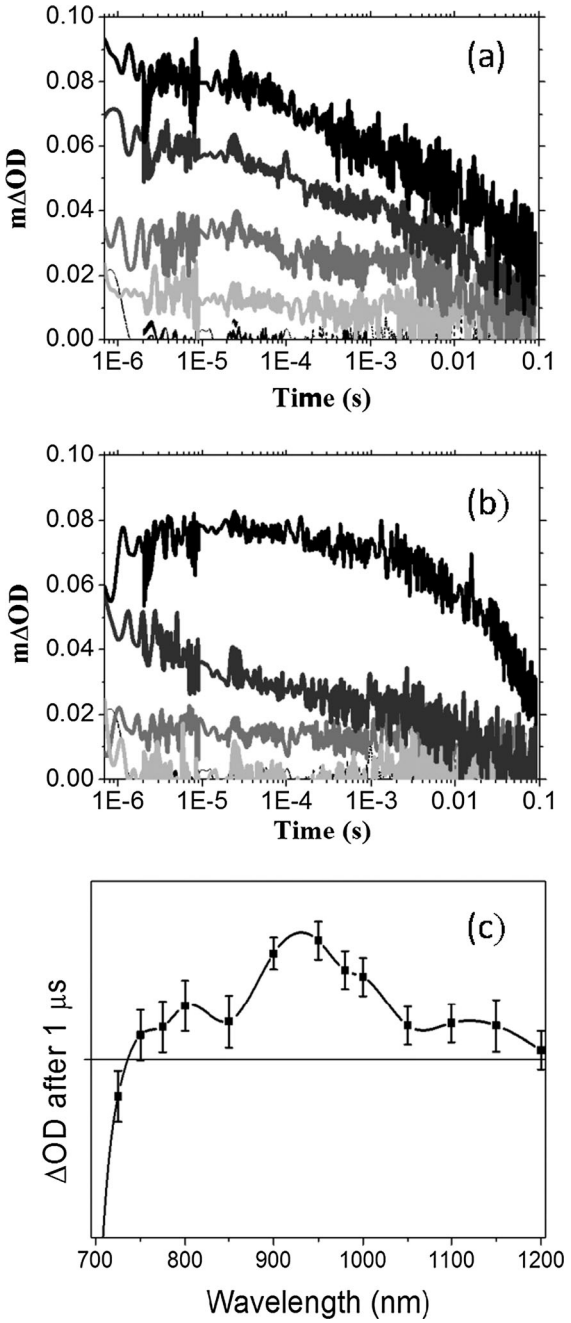

Fig. 4 Transient kinetic traces (following photoexcitation at 510 nm, pump intensity ~59 μJ cm^{-2}) of hybrid films of (a) P3HT:aerogel or (b) P3HT:QDs, with (···) 0 wt%, (—) 50 wt%, (—) 67 wt%, (—) 80 wt% and (—) 90 wt% of CdSe(ZnS). Data have been scaled by the fraction of photons absorbed at the pump wavelength. Transient absorption spectra (c) of a P3HT:aerogel film containing 90 wt% of CdSe@ZnS, 1 μs following photoexcitation at 510 nm (pump intensity ~50 μJ cm^{-2}).

the lifetime of the photoinduced charge separated state is extended using aerogels as electron acceptors, possibly as a consequence of the improved screening of charges in these systems (resulting from lower recombination due to the existence of a more interconnected network). At higher loadings of inorganic materials (90 wt%), the lifetime of QD samples tends to be similar to that of aerogels. These trends are in agreement with the photoelectrochemistry results.

The first attempts to make hybrid solar cells resulted in devices with poor performance, probably due to the rough and heterogeneous morphology of the aerogel films (Fig. S7, ESI†). Further studies are being performed to investigate the influence of annealing and other parameters on performance, as well as to obtain smoother hybrid films (*e.g.*, by incorporating the polymer *in situ* in the synthesis of the aerogels).

Conclusions

CdSe(ZnS) core(shell) aerogels were mixed with P3HT and investigated for the first time using photoelectrochemistry and transient absorption spectroscopy. Compared to organically capped, physically aggregated quantum dots, the aerogels showed increased photocurrent and charge generation in films containing lower loadings of inorganic material in combination with P3HT. The results presented here suggest that chalcogenide aerogels are suitable candidates for optoelectronic devices, especially in applications where low amounts of inorganic phase are desired.

Acknowledgements

JND and AFN thank FAPESP (2009/15428-0), CNPq and INEO for financial support. SAH acknowledges the Royal Society and UK Engineering and Physical Sciences Research Council (EPSRC) for financial support. This material is based on work supported as part of Revolutionary Materials for Solid State Energy Conversion, an Energy Frontier Research Center funded by the U.S. Department of Energy, Office of Science, and Office of Basic Energy Sciences under Award no. DE-SC0001054; and also by the National Institutes of Health, National Cancer Institute (R44 CA138013-03) *via* a subcontract from Weinberg Medical Physics, LLC (LK, SLB). Electron microscopy was acquired in the WSU Lumigen Instrument Center on a JEOL 2010 purchased under NSF Grant DMR-0216084.

Notes and references

1 Y. Liang, Z. Xu, J. Xia, S.-T. Tsai, Y. Wu, G. Li, C. Ray and L. Yu, *Adv. Mater.*, 2010, **22**, E135.
2 J. Y. Kim, K. Lee, N. E. Coates, D. Moses, T. Q. Nguyen, M. Dante and A. J. Heeger, *Science*, 2007, **317**, 222.
3 W. U. Huynh, J. J. Dittmer and A. P. Alivisatos, *Science*, 2002, **295**, 2425.
4 N. C. Greenham, X. Peng and A. P. Alivisatos, *Phys. Rev. B: Condens. Matter Mater. Phys.*, 1996, **54**, 17628.
5 E. Arici, H. Hoppe, F. Schäffler, D. Meissner, M. A. Malik and N. S. Sariciftci, *Thin Solid Films*, 2004, **451–452**, 612.
6 S. A. McDonald, G. Konstantatos, S. Zhang, P. W. Cyr, E. J. D. Klem, L. Levina and E. H. Sargent, *Nat. Mater.*, 2005, **4**, 138.
7 D. H. Cui, J. Xu, T. Zhu, G. Paradee, S. Ashok and M. Gerhold, *Appl. Phys. Lett.*, 2006, **88**, 183111.
8 S. Dayal, N. Kopidakis, D. C. Olson, D. S. Ginley and G. Rumbles, *Nano Lett.*, 2009, **10**, 239.
9 Y. F. Zhou, M. Eck, C. Veit, B. Zimmermann, F. Rauscher, P. Niyamakom, S. Yilmaz, I. Dumsch, S. Allard, U. Scherf and M. Krüger, *Sol. Energy Mater. Sol. Cells*, 2011, **95**, 1232.
10 Y. Wu and G. Q. Zhang, *Nano Lett.*, 2010, **10**, 1628.
11 B. Sun, H. J. Snaith, A. S. Dhoot, S. Westenhoff and N. C. Greenham, *J. Appl. Phys.*, 2005, **97**, 014914.
12 N. Radychev, I. Lokteva, F. Witt, J. Kolny-Olesiak, H. Borchert and J. Parisi, *J. Phys. Chem. C*, 2011, **115**, 14111.

13 J. Seo, W. J. Kim, S. J. Kim, K.-S. Lee, A. N. Cartwright and P. N. Prasad, *Appl. Phys. Lett*., 2009, **94**, 133302.
14 Y. F. Zhou, F. S. Riehle, Y. Yuan, H.-F. Schleiermacher, M. Niggemann, G. A. Urban and M. Krüger, *Appl. Phys. Lett*., 2010, **96**, 013304.
15 S. Dayal, N. Kopidakis, D. C. Olson, D. S. Ginley and G. Rumbles, *J. Am. Chem. Soc*., 2009, **131**, 17726.
16 S. Dowland, T. Lutz, A. Ward, S. P. King, A. Sudlow, M. S. Hill, K. C. Molloy and S. A. Haque, *Adv. Mater*., 2011, **23**, 2739.
17 H. C. Leventis, S. P. King, A. Sudlow, M. S. Hill, K. C. Molloy and S. A. Haque, *Nano Lett*., 2010, **10**, 1253.
18 L. X. Reynolds, T. Lutz, S. Dowland, A. MacLachlan, S. King and S. A. Haque, *Nanoscale*, 2012, **4**, 1561.
19 J. N. de Freitas, I. R. Grova, L. C. Akcelrud, E. Arici, N. S. Sariciftci and A. F. Nogueira, *J. Mater. Chem*., 2010, **20**, 4845.
20 I. U. Arachchige and S. L. Brock, *J. Am. Chem. Soc*., 2007, **129**, 1840.
21 J. L. Mohanan, I. U. Arachchige and S. L. Brock, *Science*, 2005, **307**, 397.
22 L. H. Qu and X. Z. Peng, *J. Am. Chem. Soc*., 2002, **124**, 2049.
23 M. A. Hines and P. Guyot-Sionnest, *J. Phys. Chem*., 1996, **100**, 468.
24 I. R. Pala, I. U. Arachchige, D. G. Georgiev and S. L. Brock, *Angew. Chem., Int. Ed*., 2010, **49**, 3661.
25 J. L. Mohanan and S. L. Brock, *J. Sol–Gel Sci. Technol*., 2006, **40**, 341.
26 W. W. Yu, L. Qu, W. Guo and X. Peng, *Chem. Mater*., 2003, **15**, 2854.
27 J. Jasieniak, L. Smith, J. van Embden, P. Mulvaney and M. Califano, *J. Phys. Chem. C*, 2009, **113**, 19468.
28 I. U. Arachchige and S. L. Brock, *Acc. Chem. Res*., 2007, **40**, 801.
29 M. Y. Chiu, C. C. Chen, J. T. Sheu and K. H. Wei, *Org. Electron*., 2009, **10**, 769.
30 K. Kumari, S. Chand, P. Kumar, S. N. Sharma, V. D. Vankar and V. Kumar, *Appl. Phys. Lett*., 2008, **92**, 263504.
31 J. Albero, E. Martínez-Ferrero, J. Ajuria, C. Waldauf, R. Pacios and E. Palomares, *Phys. Chem. Chem. Phys*., 2009, **11**, 9644.
32 R. Osterbacka, C. P. An, X. M. Jiang and Z. V. Vardeny, *Science*, 2000, **287**, 839.
33 M. Westerling, R. Osterbacka and H. Stubb, *Phys. Rev. B: Condens. Matter Mater. Phys*., 2002, **66**, 165220.
34 T. M. Clarke, A. M. Ballantyne, J. Nelson, D. D. C. Bradley and J. R. Durrant, *Adv. Funct. Mater*., 2008, **18**, 4029.
35 S. Dayal, N. Kopidakis and G. Rumbles, *Faraday Discuss*., 2012, **155**, 323.

